

UNIVERSIDAD SAN FRANCISCO DE QUITO USFQ

Colegio de Ciencias e Ingenierías

Diseño y Desarrollo de un Sensor de Fuerza de Seis Grados de Libertad

**Xavier Sebasitán Aguirre Lasso
Oswin Marcelino Crespo Jijón
David Andrés Molina Proaño**

Ingeniería Mecánica

Trabajo de fin de carrera presentado como requisito
para la obtención del título de
Ingenieros Mecánicos

Quito, 13 de mayo de 2020

UNIVERSIDAD SAN FRANCISCO DE QUITO USFQ

Colegio de Ciencias e Ingenierías

**HOJA DE CALIFICACIÓN
DE TRABAJO DE FIN DE CARRERA**

Diseño y Desarrollo de un Sensor de Fuerza de Seis Grados de Libertad

Xavier Sebastián Aguirre Lasso

Oswin Marcelino Crespo Jijón

David Andrés Molina Proaño

Nombre del profesor, Título académico

**Patricio Chiriboga, PhD. Vibraciones,
Delft University of Technology**

Quito, 13 de mayo de 2020

DERECHOS DE AUTOR

Por medio del presente documento certifico que he leído todas las Políticas y Manuales de la Universidad San Francisco de Quito USFQ, incluyendo la Política de Propiedad Intelectual USFQ, y estoy de acuerdo con su contenido, por lo que los derechos de propiedad intelectual del presente trabajo quedan sujetos a lo dispuesto en esas Políticas.

Asimismo, autorizo a la USFQ para que realice la digitalización y publicación de este trabajo en el repositorio virtual, de conformidad a lo dispuesto en el Art. 144 de la Ley Orgánica de Educación Superior.

Nombres y apellidos: Xavier Sebatían Aguirre Lasso

Código: 00131405

Cédula de identidad: 1723940100

Nombres y apellidos: Oswin Marcelino Crespo Jijón

Código: 00131617

Cédula de identidad: 0803760529

Nombres y apellidos: David Andrés Molina Proaño

Código: 00131740

Cédula de identidad: 1718025040

Lugar y fecha: Quito, mayo de 2020

ACLARACIÓN PARA PUBLICACIÓN

Nota: El presente trabajo, en su totalidad o cualquiera de sus partes, no debe ser considerado como una publicación, incluso a pesar de estar disponible sin restricciones a través de un repositorio institucional. Esta declaración se alinea con las prácticas y recomendaciones presentadas por el Committee on Publication Ethics COPE descritas por Barbour et al. (2017) Discussion document on best practice for issues around theses publishing, disponible en <http://bit.ly/COPETHeses>.

UNPUBLISHED DOCUMENT

Note: The following capstone project is available through Universidad San Francisco de Quito USFQ institutional repository. Nonetheless, this project – in whole or in part – should not be considered a publication. This statement follows the recommendations presented by the Committee on Publication Ethics COPE described by Barbour et al. (2017) Discussion document on best practice for issues around theses publishing available on <http://bit.ly/COPETHeses>.

1. SUMMARY

The following project discusses the preliminary steps, analysis and required work to design and manufacture a 6-axis strain gauge drive, force/torque sensor with the lowest number of strain gauges. Necessary modifications were made due to the COVID-19 health crisis that resulted in more detailed Finite Element Analysis (FEA) simulations instead of the construction of the sensor. This in return provided great feedback and a clear path for future work before proceeding with construction of the sensor as originally planned. The document will discuss the design and material selection, simulation settings, analysis of the ability of the sensor to predict load and future required work; while considering elements such as an economic factor, availability of necessary supplies, design for manufacture and the required specifications.

The first major result obtained from the study was the material used to develop the sensor. For the feasibility of the project, material availability was a crucial step since the required aluminum ingot is not a common element to obtain in Ecuador. Nevertheless, the FEA analysis and the coupled behavior of the General Calibration Matrix Cg (indicator that shows the ability of the sensor to predict loads with little disturbance from unactivated axes) showed that the steel 1045 that can be found in different suppliers locally can be used to manufacture the sensor.

After this, an analysis of the best suitable data collection equipment was done. This section concluded that, considering the nature of the project as an academic effort, laboratory equipment of the university such as a National Instruments DAQ can be implemented to detect precise and consistent results with no major electronic development. The strain gauge array and the selected data collection software will only need an external half Wheatstone bridges to work properly. If the future work is continued in an environment where the mentioned equipment isn't available the recommendations are two: check with the material science laboratory a specific strain gauge data collection card that is commonly used in material mechanics laboratory practices or have another team develop alongside a precise and consider PCB and LabView/MATLAB implementation in order to obtain precise and consistent data.

The required modifications resulted in a more detailed FEA. This study manages to optimize the best parameters to obtain the best report possible with the used software. This allowed to implement minor design changes to maintain the safety factor within the desired range while allowing the most amount of bending. This was done in order to increase the reading value the strain gauges will measure for this first functional prototype. In addition, the precise strain results of the FEA allowed to proceed with the strain gauge reduction process. This consisted in a study to reduce the maximum number of strain gauges while preserving the best level of load predictivity as the original array.

To study more in depth the level of load predictivity of the sensor the indicator cross-coupling error was introduced. This measure shows the ability of the sensor to read a load applied in a specific axis while ignoring minor effect on the rest of the axes, this is the most important indicator in the project since it will show how effective and precise is the sensor to read loads. The original strain gauge array is taken from *Shape optimization of a mechanically decoupled six-axis force/torque sensor* (Kang et al., 2014) and uses 24 strain measurement

positions. The reduction was carried out resulting in a 14-strain gauge array without changing the cross-coupling error comparing it to the original array. This was a breakthrough since it reduces significantly development costs and gives design freedom because of the reduction in the physical space used by the gauges.

With the final strain gauge array in place and the General Calibration Matrix obtained static stress FEA were performed with the six types of loads and different magnitudes to simulate real strain gauge readings. Then, with the calibration matrix constant and the strain FEA results for each load the force vector was reconstructed and verified with the load used to set up the study. The results of the study were as expected according the cross-coupling error calculated. There was an interference for the study of the Moment in X direction with the resulting force in the Z axis. Meanwhile the rest of loads were able to be reconstructed with minor interference. A study of the of the data was conducted to try to correct the error by considering the negative strain from the shear stress, solving the issue. However, considering that the gauges are only able to read compression and tension, this solution will not be physically applicable to the sensor. The investigation ended by having a CAD design of a sensor with a cross coupling error close to 20%, an optimized FEA study, the best manufacturing method for the sensor, considering the available resources, for a first functional prototype, a safe and reliable method to collect the data and a reduction in the number of strain gauges used. The next step to follow should be a reduction of the cross-coupling error in order to proceed with manufacture with the implementation of a shape optimization study. The first iteration of this study was done manually an allowed to reduce the cross-coupling error from 20% to 10%. This result is very promising and remarks the importance of this procedure to reduce the error on the sensor. Manufacture can advance to check the principle of functioning but an unoptimized sensor will not get precise results under pure loads and under combined load the error will increase, creating more complications. Shape optimization is a vital and crucial step that will enable the designed sensor to deliver the engineering requirements.

2. ABSTRACT

High precision torque and force sensors are equipment used in large branches of industry. Examples of this are robotic sensors for control and biomechanical analysis. These are expensive elements with starting prices over the thousands of American dollars which makes them inaccessible to various research centers. Moreover, there has been a great deal of research effort to develop 6 degree of freedom torque and force sensors by different teams. These groups use mostly aluminum for the metallic body of the sensor. When this material is elastically deformed by a load, it allows to perform strain measurements through deformation. This data in return, allows to reconstruct the applied load. The following study presents the analysis required for the construction of a 6-degree-of-freedom load sensor in Ecuador. The paper not only has a technical nature but considers different factors to achieve the manufacture of the product. Research showed that the mesh definition used to obtain the General Calibration Matrix is crucial to the procedure and pointed out a mesh refinement to be imperative. Also, steel was defined as the material to build the sensor's body as data confirmed no major advantage of using aluminum. In addition, the total number of occupied strain gauges was reduced from 24 to 14, causing cost savings in development and production. However, the cross-coupling error presented by the General Calibration Matrix could not be decreased from 20% without a shape optimization. Lastly, the ability of the sensor to reconstruct applied loads was evaluated by means of a Finite Element Analysis and after the inspection of the report, it was determined that the only way to decrease the sensor's error is through a parameterized optimization of its geometry combining it with static stress simulations. The first manual iteration of this procedure allowed to reduce the coupling error to a 10.0%. Therefore, the recommended future work before proceeding with manufacture is to perform such optimization.

Keywords: force, torque, sensor, gauge, strain, tension, compression, CAD, FEA, cross-coupling.

3. TABLA DE CONTENIDO

1. SUMMARY.....	5
2. ABSTRACT.....	7
3. TABLA DE CONTENIDO.....	8
4. ÍNDICE DE TABLAS.....	9
5. ÍNDICE DE FIGURAS.....	10
6. INTRODUCTION.....	11
6.1 Problem statement.....	11
6.2 Requirements List and Engineering Criteria.....	12
6.3 Requirements List and Engineering Criteria.....	13
6.4 Terms Definition.....	15
7. METHODS AND RESULTS.....	15
7.1 Overview Milestone I – Mesh Optimization.....	16
7.2 Overview Milestone II – Coupling Behavior.....	18
7.3 Overview Milestone III – Measuring Positions.....	20
7.4 Overview Experiment-Loading Tests.....	22
8. CONCLUSION.....	24
8.1 Conclusions- Mesh Optimization.....	24
8.2 Conclusions- Coupling Behavior.....	25
8.3 Conclusions- Measuring Positions.....	25
8.4 Conclusions- Loading Tests.....	26
8.5 General Conclusion.....	26
8.6 Future work.....	28
9. BIBLIOGRAPHIC REFERENCES.....	30
10. ANNEX A – STEEL BODY BLUEPRINT.....	31
11. ANNEX B – STRAIN GAUGES ASSEMBLY BLUEPRINT.....	32
12. ANNEX C: MATLAB SCRIPT-REFINED PARABOLIC STUDY Cg MATRIX.....	33
13. ANNEX D: ESTIMATED FULL BUDGET.....	35

4. ÍNDICE DE TABLAS

Table #1: Requirements and project criteria	12
Table #2: Load characteristics criteria	12
Table #3 Scaled General Calibration Matrix- Refined Parabolic Element (Milestone I)	18
Table #4 General Calibration Matrix- Steel Design 5 Measuring Pts (Milestone II)	20
Table #5 General Calibration Matrix for 14 Strain Gauges (milestone III)	21
Table # 6 Comparison of CC error, before and after shape optimization	29

5. ÍNDICE DE FIGURAS

Figure #1 First Layout Defined for Strain Gauges	13
Figure #2 Linear Tetrahedron element	16
Figure #3 Parabolic Tetrahedron element	16
Figure #4 Convergence Plot (added-fillet design)	17
Figure #5 Measuring Points Diagram (dimensions in mm)	19
Figure #6 Layout of the system with 14 strain gauges	21
Figure #7 Plot of results for Loading Tests F_x	23
Figure #8 Example of the behavior obtained for loads in M_x	23
Figure # 9 First Shape optimization Performed	28

6. INTRODUCTION

The following project was developed in Quito, Ecuador as a graduation project for the Mechanical Engineering degree. The investigation consists in the design and development of a 6-DOF (degree of freedom) force and torque sensor under Ecuador's situation and possibilities. This means that the sensor must read and report values of both force and torque in the three main cartesian axes X , Y and Z , resulting in 6 reported values. The mentioned project had available approximately 5 months for its development and was directed for the Biomechanical Research and Development Department of the Universidad San Francisco de Quito.

The main objectives determined for the development of this project were the definition of the best design of the geometry of the sensor, using performance optimization as the main criterion; designate the manufacturing process, simulate a functioning sensor prototype and contribute to the development of Biomechanics and Robotics in the Universidad San Francisco de Quito and consequently, in Ecuador.

6.1 Problem statement

The study of biomechanics and robotics require data gathering through numerous sources, such as sensors. For motion study specifically, 6 degrees of freedom sensors (6 DOF Sensors) are vital for data collection. For this reason, this type of sensors is needed in the Biomechanics and Robotics Laboratory of the Universidad San Francisco de Quito for the development of projects, such as prosthetics and robotic arms. The need mentioned is aggravated by the lack

of suppliers in Ecuador to provide this equipment and the high cost of this technology in the market.

6.2 Requirements List and Engineering Criteria

Defining the base parameters of the investigation is crucial during project development. This process allows for needs to be translated into a measurable language to start the development process.

Requirements List	Engineering Criteria
Obtain a calibration matrix with a minimal cross coupling error	<i>Cross – coupling error $\leq 5\%$</i>
Obtain efficient and accurate meshing	<i>Convergence error $\leq 5\%$</i>
Use as few strain gages as possible	<i>Total number of gauges ≤ 24</i>
Report accurately applied loads	$\Delta F \leq 5\%$
It must be possible to manufacture in Ecuador	<i>Availability of 80% of the pieces locally</i>

Table #1: Requirements and project criteria

Load characteristics						
Load direction	F_x	F_y	F_z	M_x	M_y	M_z
Maximum applied force and moment	2500 N	2500 N	4500 N	100 Nm	100 Nm	100 Nm
Resolution	± 0.1 N	± 0.1 N	± 0.1 N	± 0.005 Nm	± 0.05 Nm	± 0.005 Nm

Table #2: Load characteristics criteria

6.3 Requirements List and Engineering Criteria

Several crucial parameters were defined. The layout for the strain gauges is shown below:

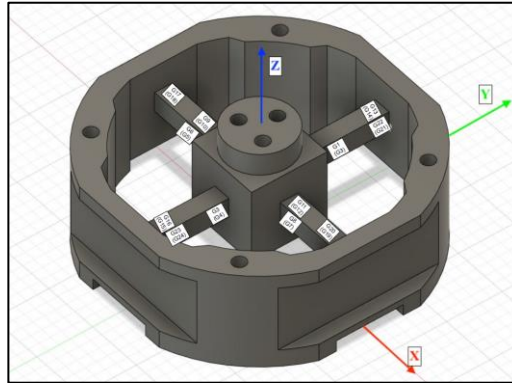


Figure #1 First Layout Defined for Strain Gauges

The equation needed to obtain force/torque data from the strain gauges follows along with an explanation for each term:

$$\vec{F} = C_g \times \vec{\epsilon}$$

Data from the strain will be organized in the $\vec{S}_{6 \times 1}$ vector defined below:

$$\vec{S} = \frac{1}{4} \times \begin{bmatrix} \epsilon_1 - \epsilon_2 + \epsilon_3 - \epsilon_4 \\ \epsilon_5 - \epsilon_6 + \epsilon_7 - \epsilon_8 \\ \epsilon_9 - \epsilon_{10} + \epsilon_{11} - \epsilon_{12} \\ \epsilon_{13} - \epsilon_{14} + \epsilon_{15} - \epsilon_{16} \\ \epsilon_{17} - \epsilon_{18} + \epsilon_{19} - \epsilon_{20} \\ \epsilon_{21} - \epsilon_{22} + \epsilon_{23} - \epsilon_{24} \end{bmatrix} = \begin{bmatrix} S_{F_x} \\ S_{F_y} \\ S_{F_z} \\ S_{M_x} \\ S_{M_y} \\ S_{M_z} \end{bmatrix}$$

The strain numbering corresponds to each strain gauge in the layout figure above, for example gauge $G1$ reports strain ϵ_1 .

The matrix $E_{6 \times 6}$ is defined as a concatenation of \vec{S}_j vectors obtained from applying the corresponding equations to 6 different cases of pure load.

$$E = \begin{bmatrix} S_{11} & S_{12} & S_{13} & S_{14} & S_{15} & S_{16} \\ S_{21} & S_{22} & S_{23} & S_{24} & S_{25} & S_{26} \\ S_{31} & S_{32} & S_{33} & S_{34} & S_{35} & S_{36} \\ S_{41} & S_{42} & S_{43} & S_{44} & S_{45} & S_{46} \\ S_{51} & S_{52} & S_{53} & S_{54} & S_{55} & S_{63} \\ S_{61} & S_{62} & S_{63} & S_{64} & S_{65} & S_{66} \end{bmatrix}$$

The matrix $D_{6 \times 6}$ is defined with the reciprocals of the pure loads applied as the main diagonal of the matrix:

$$D = \begin{bmatrix} \frac{1}{F_x} & 0 & 0 & 0 & 0 & 0 \\ 0 & \frac{1}{F_y} & 0 & 0 & 0 & 0 \\ 0 & 0 & \frac{1}{F_z} & 0 & 0 & 0 \\ 0 & 0 & 0 & \frac{1}{M_x} & 0 & 0 \\ 0 & 0 & 0 & 0 & \frac{1}{M_y} & 0 \\ 0 & 0 & 0 & 0 & 0 & \frac{1}{M_z} \end{bmatrix}$$

The matrix $C_{g_{6 \times 6}}$ is defined as the multiplication of the inverse of the matrixes E and D .

$$C_g = E^{-1} \times D^{-1}$$

6.4 Terms Definition

- 6 DOF Load Sensor: sensor with the ability to read and report values of both force and torque in the three main cartesian axes, resulting in 6 reported values
- Applied Load: force and moment that are applied to the sensor
- Cross-coupling error: ability of the sensor to isolate an applied load in a specific axis and read it without disturbance of the effect that the rest of the axis have on the measurement.
- CAD: computer aided design used to generate 3D models through a computer software
- FEA: finite element analysis used to solve and simulate mechanical studies.
- General Calibration Matrix: constant matrix dependent on the geometry of the sensor that when multiply by deformation readings, obtain when a load is applied, it reconstructs the original applied load.
- Decoupled matrix: a type of square matrix with high values in the main diagonal and with all zeroes off-diagonal values.

Below is the method and results section, which will present the experiments and studies that were carried out for this project and the results obtained.

7. METHODS AND RESULTS

The following section will gather and summarize the most relevant data obtained from each milestone simulation run throughout the investigation. Each study is briefly explained along with the results employed to progressively improve the sensors accuracy.

7.1 Overview Milestone I – Mesh Optimization

For the first milestone there was the need, through a FEA (Finite Element Analysis), to optimize the mesh settings in order to obtain the most decoupled General Calibration Matrix. The study compared different types of tetrahedral elements and the impact of refinement on the General Calibration Matrix. This study allowed to properly define the required FEA settings to obtain the best possible results while preserving computation time (computation time didn't had a major impact on our investigation but it is vital step when performing a shape optimization analysis which is recommended to do before proceeding with construction).

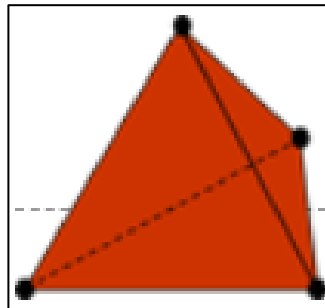


Figure #2 Linear Tetrahedron element

Source: Autodesk Knowledge

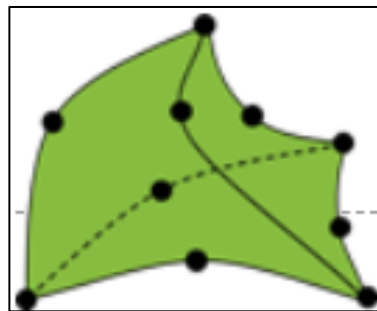


Figure #3 Parabolic Tetrahedron element

Source: Autodesk Knowledge

Hexahedral elements were not used in the investigation since reports show there is no clear advantage between hexahedral and tetrahedral for this type of static stress simulation (Wang et al., 2004).

At the end of this analysis the defined settings of the best possible mesh were: using a parabolic tetrahedral element, proceeded with mesh refinement analysis until convergence, through this results continue with minor changes in the design like fillets and thicker walls and finally run the simulation again. These steps gave us the best possible FEA for the needs of the project. These changes resulted in a General Calibration Matrix with a more decoupled behavior.

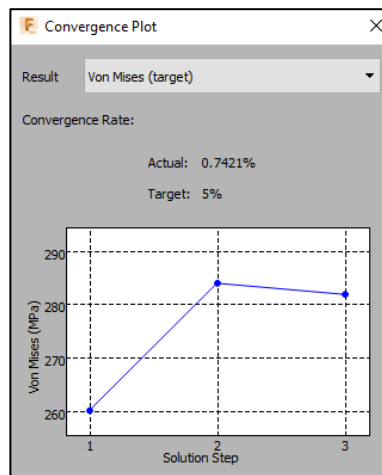


Figure #4 Convergence Plot (added-fillet design)

$C_{g_{Refined}}/10\ 000$ (24 strain gauges)					
820	1	-1	12	13	-6
-2	817	1	4	180	-32
-83	-78	658	-144	-26	-334
-1	-3	4	334	0	2
0	0	2	-7	339	-3
0	-1	0	1	1	407

Table #3 Scaled General Calibration Matrix- Refined Parabolic Element (Milestone I)

7.2 Overview Milestone II – Coupling Behavior

The second milestone had 2 main goals. The first one was to redesign a sensor using Aluminum 6061 since it is a common material seen in different papers such as *Novel Strain Gauge Arrangement and Error Reduction Techniques* (Kebede et al., 2019) and *Shape optimization of a mechanically decoupled six-axis force/torque sensor* (Kang et al., 2014). This procedure was performed to verify how the properties of the construction material could affect the system's General Calibration Matrix. Then, such matrix for Aluminum 6061 was obtained and compared with the matrix of the Steel AISI 1045 sensor design in order to check if varying the material could significantly affect the calibration matrix. Finally, the second goal was to decrease the percentage of difference in each column of the General Calibration Matrix through

a strain area analysis instead of a singular strain measurement on the FEA results. This was done on the study of the selected material.

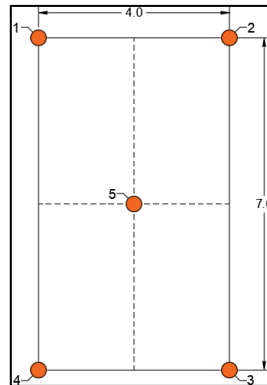


Figure #5 Measuring Points Diagram (dimensions in mm)

Due to its price, availability on the country and since the results of the FEA analysis had very small variations when comparing the 2 materials and considering the required specifications by the client, the Steel design sensor was selected. This does not mean a different material shouldn't be consider since material selection must be analyzed for each specific case and not general use when developing this type of sensors. Then, instead of using a singular measuring point of strain in the FEA results, five strain readings were considered for each strain gauge measurement position in order to obtain an average strain. This method resulted in a lower percentage of difference in each column for the General Calibration Matrix resulting in the best decoupled behavior yet without performing a shape optimization.

$C_{g_{5-pt.}}/10\ 000$ (24 strain gauges)					
1671	1	0	-3	-3	-1
0	1670	-1	-1	3	0
-149	-60	750	-59	-1	-8
0	0	0	109	0	0
0	0	0	0	109	0
-1	0	3	-1	0	183

Table #4 General Calibration Matrix- Steel Design 5 Measuring Pts (Milestone II).

7.3 Overview Milestone III – Measuring Positions

For the third milestone simulation the goal was to reduce the number of strain gauges used in the sensor while maintaining the same percentage of cross-coupling behavior. This idea provided cost savings and design liberty benefits. It was crucial since the development of this type of equipment is extremely expensive so any activity towards lowering manufacturing costs are important for its competitiveness in the market once the project is fully developed.

In order to verify if decreasing the number of strain gauges didn't had a negative impact on the precision of the sensor, a new indicator was introduced. Consider the $E_{6 \times 6}$ matrix, a row i and a column j are determined, the values in the diagonal can be then represented as e_{ii} and the other values as e_{ij} if $i \neq j$. The cross-coupling ratio is then defined as the division of the off-diagonal value in the row i by the corresponding diagonal value (Kang et al., 2014). This description is results in the following expression:

$$CC_{ij} = \frac{e_{ij}}{e_{ii}} \times 100\%$$

This indicator was the cross-coupling error, it measures the ability of the sensor to isolate and read a specific load while ignoring any sort of disturbance or effect of this load on the rest

of the axis. Meaning if a load on the positive X direction is applied, the sensor should only read the strain of the sensors for this direction and minimize deformations that are occurring in other sections of the sensor. Considering this, the cross-coupling error was analyzed until finding the lowest number of strain gauges that has no effect on comparing with the original array.

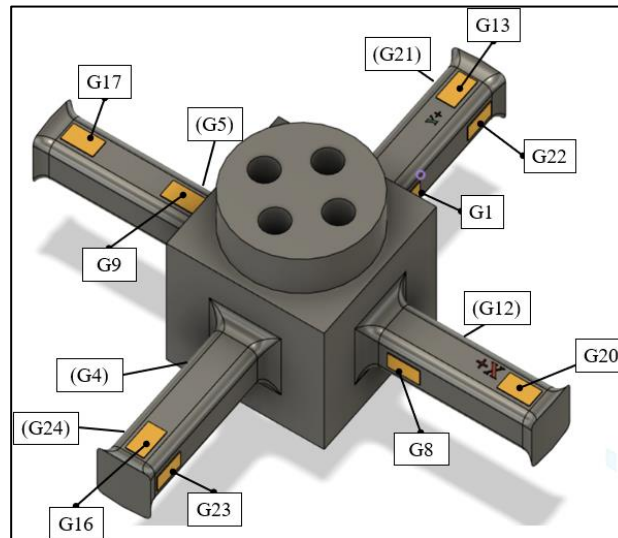


Figure #6 Layout of the system with 14 strain gauges

This procedure allowed the sensor to use a 14-strain gauge array with no effect on the sensors precision which has a major economic impact on its development.

$C_{g_{14-SG}}/10\ 000$ (14 strain gauges)					
1671	1	0	-6	-4	1
1	1669	-1	-1	2	-1
-149	-59	750	-54	34	-10
0	0	0	105	0	0
0	0	0	0	105	0
-1	0	6	-1	1	183

Table #5 General Calibration Matrix for 14 Strain Gauges (milestone III)

Below is the economic comparison made between the 2 strain gauge configurations.

Original Configuration Price = \$173.90

Optimized Configuration Price = \$101.44

Saving = 41.7%

7.4 Overview Experiment-Loading Tests

The sensor worked correctly with maximum loads and there were no variations or errors in the data obtained because the General Calibration Matrix had been calculated with these loads. To verify that the system would report the data correctly, simulations in which the sensor was loaded with pure loads with different values that would be within the operating range were performed. Afterwards, the deformation data obtained with each applied pure load was taken and the theoretical loads that would be reported by the sensor were calculated.

In order to have a better appreciation of the results obtained, graphs were drawn in which the applied loads were presented in the x axis as the independent variable and the reported loads in the y axis. In this way, it could be observed that for most cases, the loads reported were correct or had a minimum error, this error was neglected because it was caused by the decoupling behavior inherent to the design. There was an exception for the behavior of the results obtained for loads in M_x , this occurred due to the combination of different factors that will be better explained in the conclusions section.

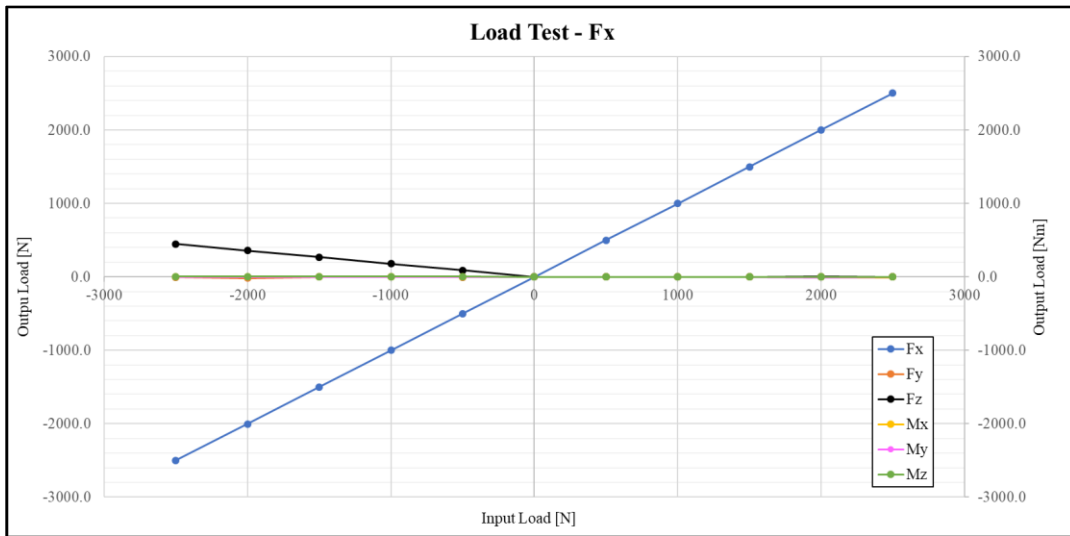


Figure #7 Plot of results for Loading Tests Fx

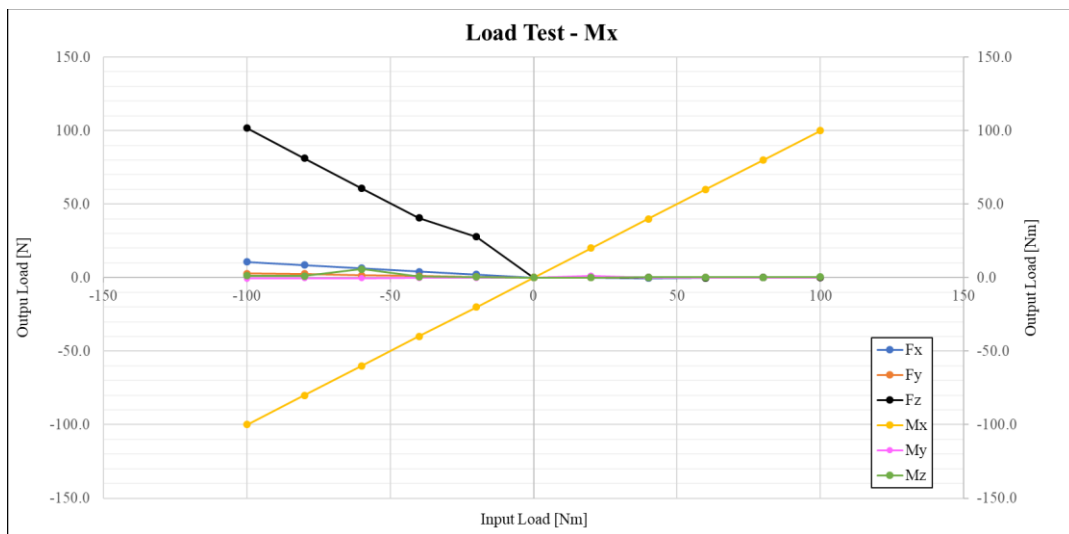


Figure #8 Example of the behavior obtained for loads in Mx

Finally, the conclusions of the project are presented in the following section, these were made based on the results obtained and the engineering criteria shown in the introductory section.

8. CONCLUSION

The following section gives conclusions obtained from the relevant results and discussions from each milestone simulation. Each study gives its conclusions along with an explanation of their overall influence on the project. Finally, a general conclusion for the project is presented.

8.1 Conclusions- Mesh Optimization

- After examining all 3 of the General Calibration Matrixes it is shown that a more refined mesh gets a more decoupled matrix which is the main objective. Having a better mesh quality is crucial for this type of analysis since the resulting strain values will allow for a functioning force/torque sensor.
- It is vital for a Finite Element Analysis study to refine the solution in places where further calculations take place. Therefore, for this investigation a local mesh and adaptive mesh refinement was needed.
- Having a singular strain measurement instead of an average strain measurement of a zone can generate flaws in the moment section of the strain matrix for the parabolic refined study.
- There is a need to be extremely careful when the element is chosen to run a Finite Element Analysis simulation, even more if the study is run through Autodesk's Fusion 360, where computation time between a linear and a parabolic tetrahedron don't differ much when solving such study in the cloud. This means, associating computation time to a quality refine mesh with more precise results is not the right choice with a cloud-based simulation motor.

8.2 Conclusions- Coupling Behavior

- There is no clear benefit relating to the behavior of the matrix from switching to a different material, coupling problem is independent of the material used for the sensor's body. This applies if the material works within the elastic zone of the stress-strain curve.
- Steel is the best material to use for manufacturing the sensor body in Ecuador because it meets the requirements of availability, price and mechanical properties that allowed to meet the needs of the sensor.
- Better results are obtained with the use of 5-point strain measurement array because an improvement of the decoupled behavior of the strain matrix is obtained, generated by using an average strain in an area instead of a single value of strain in one point.

8.3 Conclusions- Measuring Positions

- There is cost savings when using less strain gauges and design liberty since there is fewer strain gauges in the sensor.
- To reduce the CC error in the 12-strain gauge array a shape optimization study must take place.
- The 14-Strain Gauge Array is the best option for this design because the CC is not affected and remains the same compared to the original arrangement of 24 strain gauges.
- Reducing the number of strain gauges represent a cost saving of 41.7% of the original budget for strain gauges.

8.4 Conclusions- Loading Tests

- The sensor can predict pure loads in every axis without major disturbance except for the case of negative moments on the X direction.
- In the load case of negative moment in the X direction the greatest errors occur due to the addition of the Cross-coupling error and the need to use signs for torsional deformations.
- The only viable solution is to eliminate the cross-coupling error of the General Calibration Matrix through optimizations in the design.
- It is recommended to develop a six-axis force/torque sensor with shape optimization of the CAD design. This will decouple the general calibration matrix, eliminating any type of cross coupling error and thus obtaining an effective sensor.

8.5 General Conclusion

- Since the coupling behavior was determined to be better for a 5-point average strain measurement per position. Using a software that allows a shape optimization and a strain average of a specified zone might reduce the error even more.
- A quality mesh in a study with such a high sensitivity is an important step. With this said, using a software that enables cloud-based solving can reduce a great amount of time in development. This becomes especially true if a shape optimization procedure takes place.
- In this project, only the manufacturing costs of the sensor were considered, but it is important to consider that there are quite a few indirect costs if it is decided to develop

the sensor in an industrial scale. These costs relate to the equipment necessary to carry out the physical tests or the data acquisition equipment.

- The results show no major differences in the behavior of the General Calibration Matrix when comparing the aluminum and the steel bodies. This gives evidence that using aluminum for the sensor's body is not a must but a choice. Therefore, given the availability of metallic materials in Ecuador, it is highly recommended to build the sensor using steel. The benefits of making this decision are the savings in costs that would generate using steel and decreasing the general size of the sensor due to the greater capabilities of this material to withstand loads when compared to aluminum. Nevertheless, using steel increases the machining costs inevitably.
- The 14-strain gauge array was the best choice due its coupling error/economic impact vs the different analyzed strain gauges arrays. It is important to validate the ability of this array to predict loads through physical tests. Any sort of real error, once completed a shape optimization, can be tracked to this modification so it's important to compare it with different options even though in a theoretical way the reduction of gauges was approved.
- The main conclusion obtained from the project is the need for shape optimization through a Finite Element Analysis and a parametrized geometry component of the sensor. It is the only way to minimize the cross-coupling error and delivered a sensor with the required specifications. This is an important conclusion for the project since proceeding with the manufacture and having the error appear in this step is time consuming and a waste of resources if the problem can be anticipated in early stages.

8.6 Future work

The investigation planted the workflow and acquired the information needed to proceed with the fabrication of the sensor, however because of the error on the design, that can only be corrected through a shape optimization, it is not recommended to fabricate the system before such parametric shape optimization is performed on the sensor's design. This will allow for the sensor to correct the cross-coupling error and have precise results as required.

A shape optimization consists in parametrizing different geometry elements of the sensor and link them with a Finite Element Analysis (FEA). The program should consist in running a simulation and have the results calculate the cross-coupling error of the sensor under a specific load. If the cross-coupling error is outside of the desired range, as it is the case of our design, minor step changes will be done in the parametrized geometry values such as the thickness of the beams, the thickness of the walls and area of center core. Then, a different simulation should be run with the geometry changes and the cross-coupling error would be calculated. This process must be repeated in a loop until the desired cross-coupling error is achieved. To illustrate the influence of shape optimization, the first iteration was performed. The results in the cross-coupling behavior are shown below along with the illustration of the changes made.

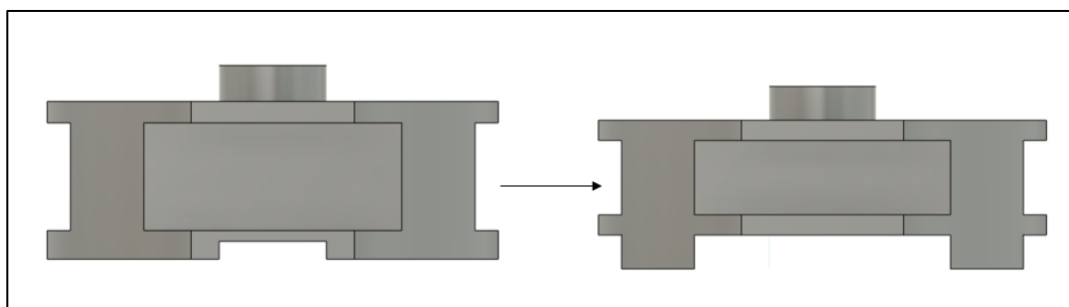


Figure # 9 First Shape optimization Performed

Cg		
Row	CC_{max} Before	CC_{max} After
1	0,3%	0,2%
2	0,1%	0,3%
3	19,9%	10,0%
4	0,2%	0,9%
5	0,4%	0,4%
6	3,4%	0,7%

Table # 6 Comparison of CC error, before and after shape optimization

Shape optimization be a thorough process regarding a FEA and will need a software that enables code to be linked with its simulation capabilities. With this said, motors such as the one found in Abaqus or Ansys might be the right decision to proceed with this task.

Once the shape optimization is completed and the sensor its ready for production, the paper has the contact information to acquire the necessary equipment such as the steel ingot, DAQ data collection system and strain gauges. These elements were considered in the city of Quito and San Francisco University because of their availability, if the sensor is desired to be manufacture in a different area one should confirm if there is access to the materials.

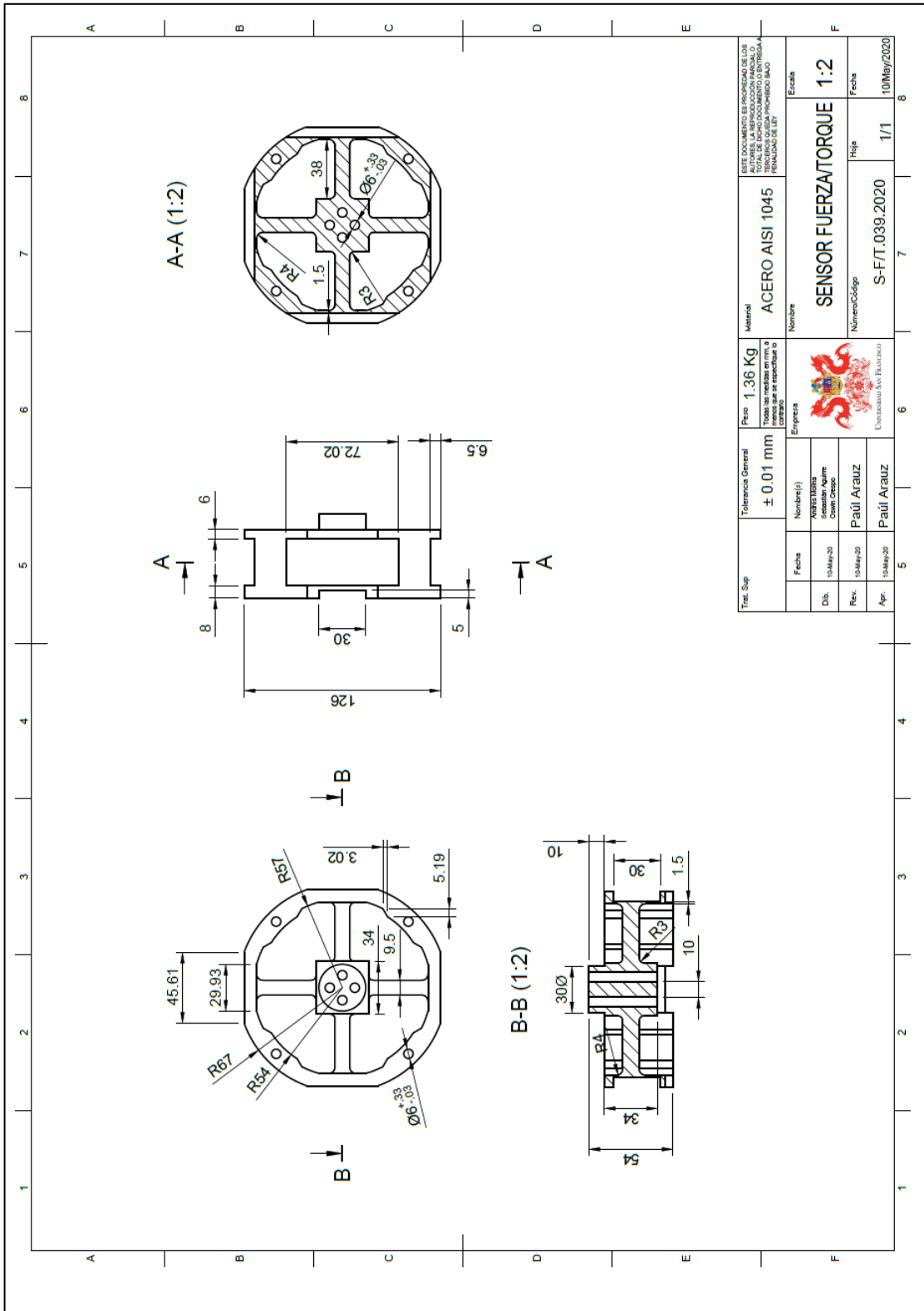
If the manufacture of the sensor is going to advance as guided in the investigation once the sensor is set up, load test should be the first required activity to validate physically the

ability of the sensor the reconstruct loads. This test should be performed with pure control loads so any sort of minor error can be calibrated, and the precision ranges are achieved.

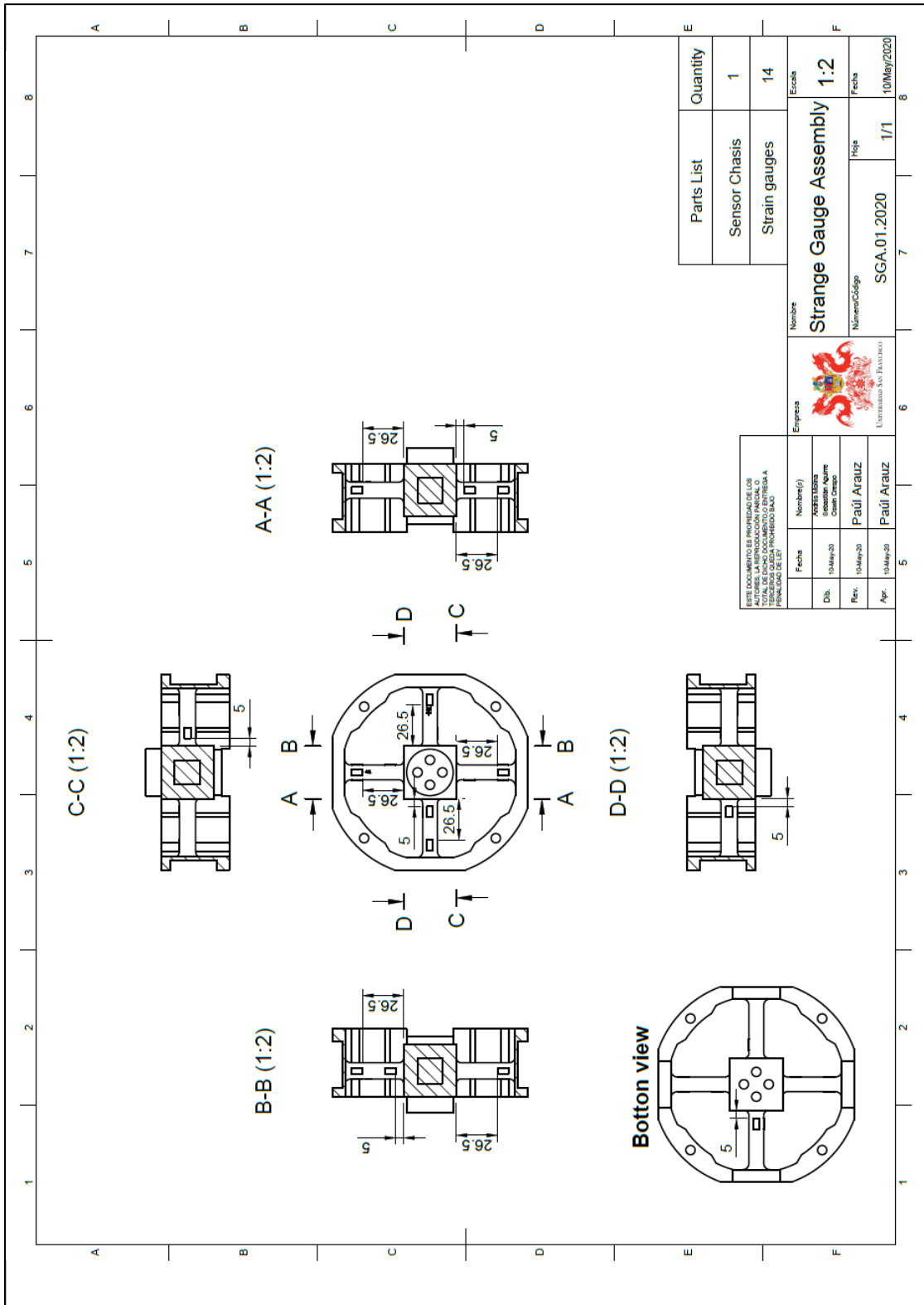
9. BIBLIOGRAPHIC REFERENCES

- Autodesk Knowledge. (n/d). *Inventor Nastran- Section 7: Meshing*. Retrieved on April 3rd, 2020 from: <https://knowledge.autodesk.com/support/inventor-nastran/getting-started/caas/CloudHelp/cloudhelp/2020/ENU/NINCAD-SelfTraining/files/GUID-2CB5E408-C795-41EE-9F83-B311BFD99FB0-htm.html>
- Kang, M. K., Lee, S., & Kim, J. H. (2014). Shape optimization of a mechanically decoupled six-axis force/torque sensor. *Sensors and Actuators, A: Physical*, 209, 41–51. <https://doi.org/10.1016/j.sna.2014.01.001>
- Kebede, G. A., Ahmad, A. R., Lee, S.-C., & Lin, C.-Y. (2019). *Novel Strain Gauge Arrangement and Error Reduction Techniques*. 5–9.
- Wang, E., Nelson, T., & Rauch, R. (2004). Back to Elements - Tetrahedra vs . Hexahedra. *CAD-FEM GmbH, Munich, Germany*, 16. <http://www.ansys.com/staticassets/ANSYS/staticassets/resourcelibrary/confpaper/2004-Int-ANSYS-Conf-9.PDF>

10. ANNEX A – STEEL BODY BLUEPRINT



11. ANNEX B – STRAIN GAUGES ASSEMBLY BLUEPRINT



12. ANNEX C: MATLAB SCRIPT-REFINED PARABOLIC STUDY CG MATRIX

```

%Recordar importar los valores primero, luego arrastrar la Tabla hasta
%Current folder
% Obtencion de los Datos
clc, clear all
format short
load StrainValuesSteel120.mat
% Recuperar los valores de Fuerza y Momento, vector con Fx, Fy, Fz, Mx, My,
% Mz
F = StrainValuesSteel120.Input(1:6);
% Valores de Deformacion para cada Strain Gage, pruebas de Fuerza
Fx = StrainValuesSteel120.Fx;
Fy = StrainValuesSteel120.Fy;
Fz = StrainValuesSteel120.Fz;
% Valores de Deformacion para cada Strain Gage, pruebas de Momento
Mx = StrainValuesSteel120.Mx;
My = StrainValuesSteel120.My;
Mz = StrainValuesSteel120.Mz;
% Se crea la matriz de deformacion para los 6 experimentos, SG
SG_Steel14SG = [ Fx, Fy, Fz, Mx, My, Mz];
%% Matrices Importantes
% Matriz de Estandarizacion, [D]
format rat
D = diag(1./F);
%% Matriz de deformacion E
format short
E_Steel14SG = zeros (6);

```

```
for i=1:6

    E_Steel14SG(1,i) = SG_Steel14SG(1,i) - SG_Steel14SG(4,i);
    E_Steel14SG(2,i) = SG_Steel14SG(5,i) - SG_Steel14SG(8,i);
    E_Steel14SG(3,i) = SG_Steel14SG(9,i) - SG_Steel14SG(12,i);
    E_Steel14SG(4,i) = SG_Steel14SG(13,i) - SG_Steel14SG(16,i);
    E_Steel14SG(5,i) = SG_Steel14SG(17,i) - SG_Steel14SG(20,i);
    E_Steel14SG(6,i) = 0.5.*(SG_Steel14SG(21,i) - SG_Steel14SG(22,i) +
    SG_Steel14SG(23,i) - SG_Steel14SG(24,i));

end

E_Steel14SG = 0.50*E_Steel14SG;
%Obtencion de la Matriz General de Calibracion
Cg_Steel14SG=(inv(D)*inv(E_Steel14SG));
```

13. ANNEX D: ESTIMATED FULL BUDGET

Main Costs					
Expenses	QTY	Total Price	Supplier	Description	Observation
Steel Ingot	1	\$42.34	IVAN BOHMAN	750 AISI 1045 Carbon Steel	An invoice with the established priced was send by the distributor
CNC Machining	1	\$220	MECANIZADO CNC	3 Axis CNC Milling	The price was established by the distributor before manufacturing and the payment is with delivery of the final product
Strain gauge	20	\$144.00	OMEGA- a Spectris company	1-axis general purpose steel-strain gauge, 350 Ω .	This is a cost applicable only to the U.S.A. area and does not consider any nationalization or tax costs to buy it in the country. The delivery should be done by a member of the group.
Industrial glue	1	\$34.48	OMEGA- a Spectris company	Methyl-based cyanoacrylate	This is a cost applicable only to the U.S.A. area and does not consider any nationalization or tax costs to buy it in the country. The delivery should be done by a member of the group.
Resistors	20	\$2.00	APM: all power microcontrollers	General purpose 350 Ω resistor.	-
Solder-able breadboard	6	\$7.50	APM: all power microcontrollers	General purpose breadboard.	-
TOTAL		\$450.32			
Unexpected Expenses		\$50			
Estimated final price		\$500.32			